Membrane-mediated Induction and Sorting of K-Ras Microdomain Signaling Platforms

Katrin Weise, [†] Shobhna Kapoor, [†] Christian Denter, [†] Jörg Nikolaus, [‡] Norbert Opitz, [§] Sebastian Koch,   Gemma Triola,   Andreas Herrmann, [‡] Herbert Waldmann, and Roland Winter [*†]

[†] Physical Chemistry I, Biophysical Chemistry, Faculty of Chemistry, TU Dortmund University.

[‡] Institute of Biology/Biophysics, Humboldt University Berlin.

[§] Max Planck Institute of Molecular Physiology, Dortmund.

 Chemical Biology, Max Planck Institute of Molecular Physiology, Dortmund and Faculty of Chemistry, TU Dortmund University.
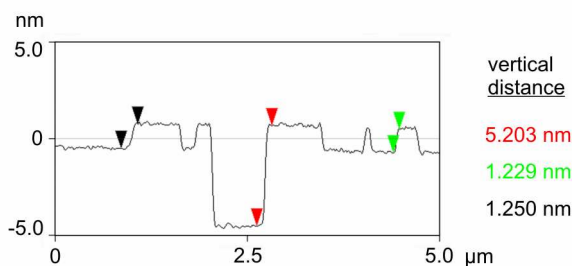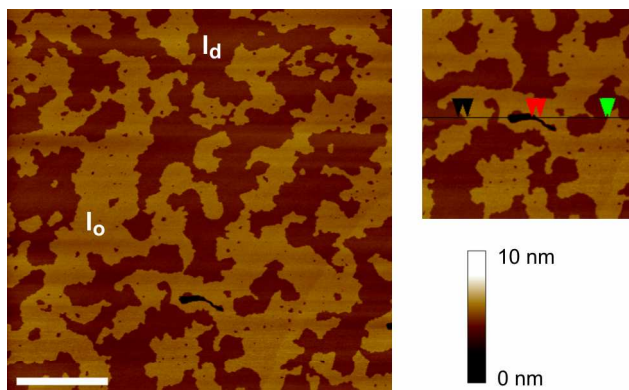
Figure S1. AFM image of a DOPC/DOPG/DPPC/DPPG/Chol 20:5:45:5:25 lipid membrane on mica. In the upper part, the whole scan area is shown with a vertical color scale from dark brown to white corresponding to an overall height of 10 nm, indicating a homogeneous lipid bilayer with coexisting domains in l_o and l_d phase. The concomitant section profile of the AFM image is given at the bottom. The horizontal black line in the figure on the right hand side is the localization of the section analysis shown at the bottom, indicating the vertical distances between pairs of arrows (black and green: height difference of the l_o/l_d phases and red: thickness of the l_o domains). The thickness of the lipid bilayer is ~5.2 nm for the l_o phase and ~4.0 nm for the l_d phase, i.e., the coexisting phases can be distinguished by a height difference of ~1.0 nm, in agreement with previous and literature data on other zwitterionic model raft mixtures.[S1,S2] The scale bar corresponds to 2 μm.
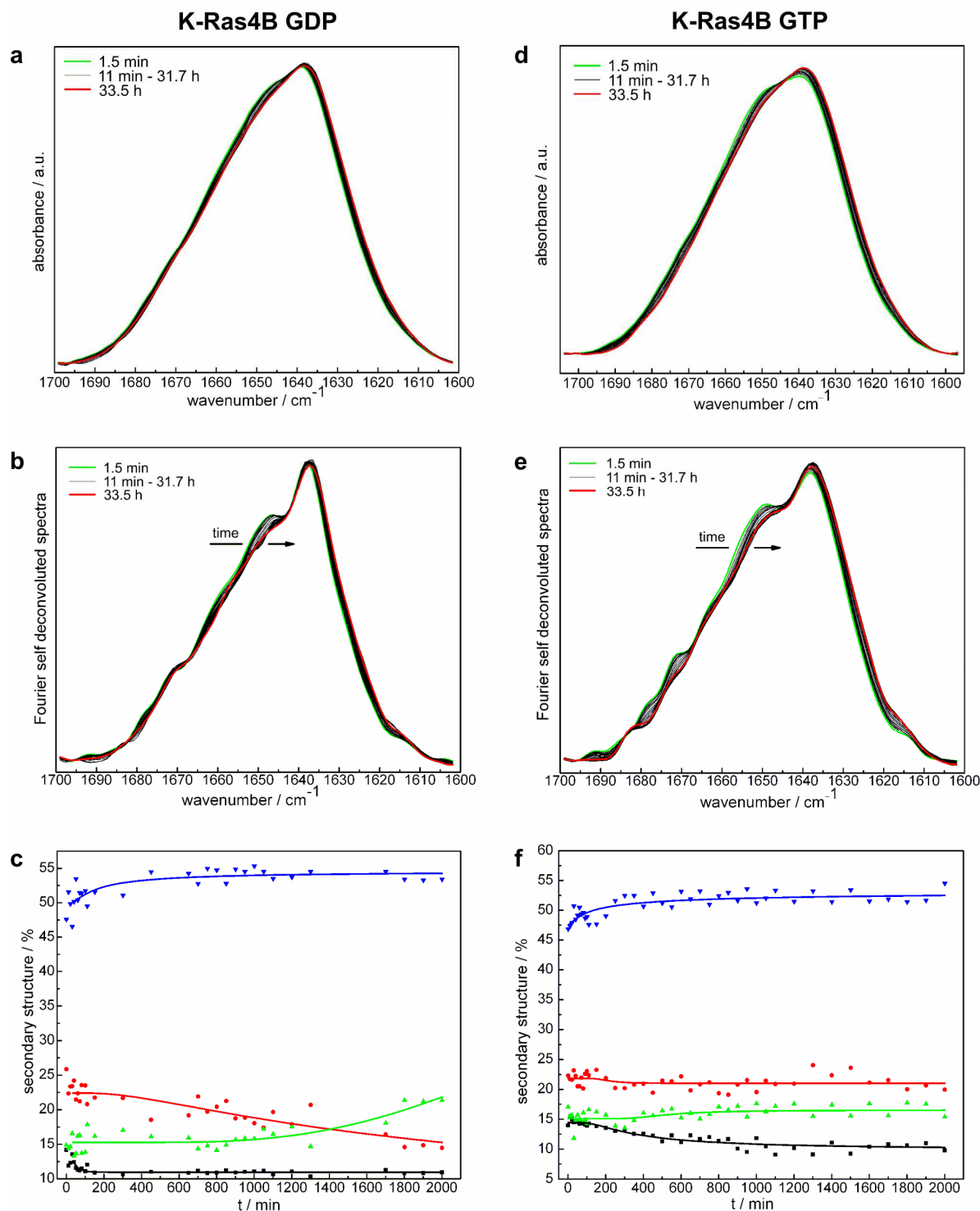
Figure S2. Structural evaluation of the GDP- and GTP-loaded K-Ras4B membrane interaction. Figures a and d show the normalized FTIR spectra and panels b and e the concomitant Fourier self deconvolution spectra of the amide-I′ bands of K-Ras4B GDP and K-Ras4B GTP in the presence of DOPC/DOPG/DPPC/DPPG/Chol 20:5:45:5:25 at 25 °C. Peak fitting of the normalized FTIR spectra yields the time evolution of the secondary structural changes of K-Ras4B GDP (c) and K-Ras4B GTP (f) in the presence of DOPC/DOPG/DPPC/DPPG/ Chol 20:5:45:5:25 at 25°C. The color code corresponds to the following wavenumbers and structural elements: ■ 1671 cm^{-1} loops, ● 1661/1654 cm^{-1} α-helix, ▲ 1647 cm^{-1} unordered structures, and ▼ 1637/1626 cm^{-1} β-sheets (intramolecular). Within the experimental error of a few %, no marked changes in secondary structure occur with time.
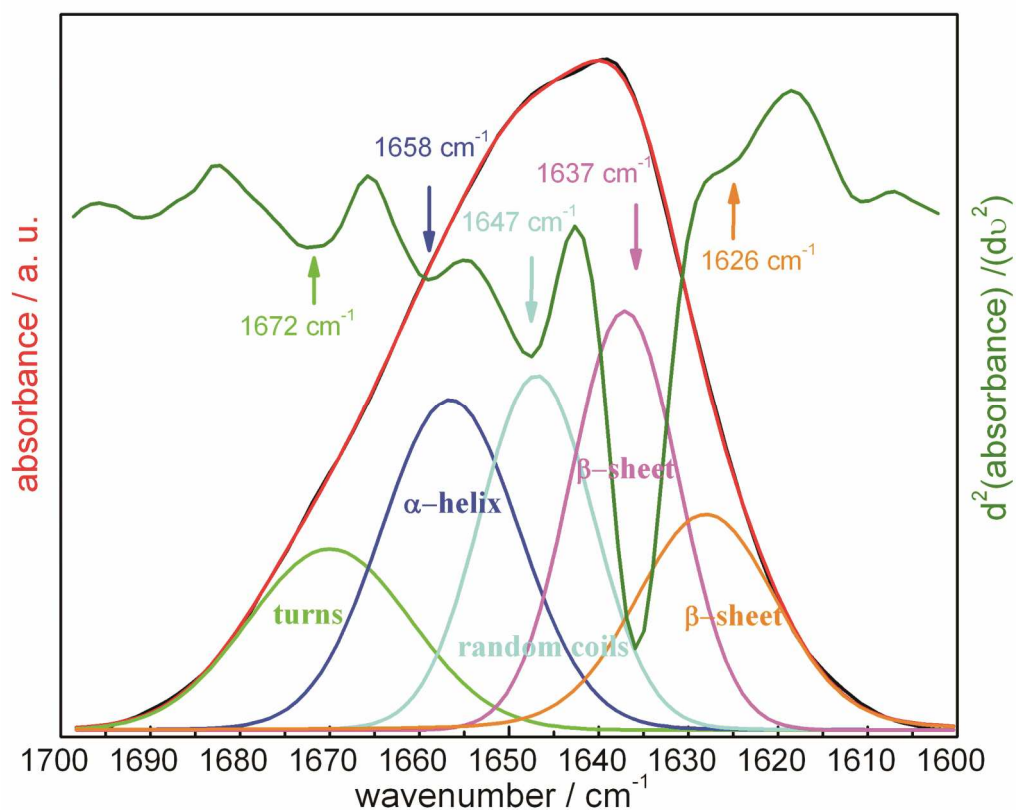
Figure S3. Structural analysis of the GDP-loaded K-Ras4B in bulk solution. The local minima and maxima from the second derivative and FSD, respectively, were used to identify the amide-I′ components at 1672, 1658, 1647, 1637, and 1626 cm^{-1}. While assigning the peaks, ambiguities such as overlap of the unordered and α-helical regions were also considered, taking also the X-ray and NMR data into account. The area under each peak represents the fraction of each component and was finally used to determine the percentages of the secondary structure components.
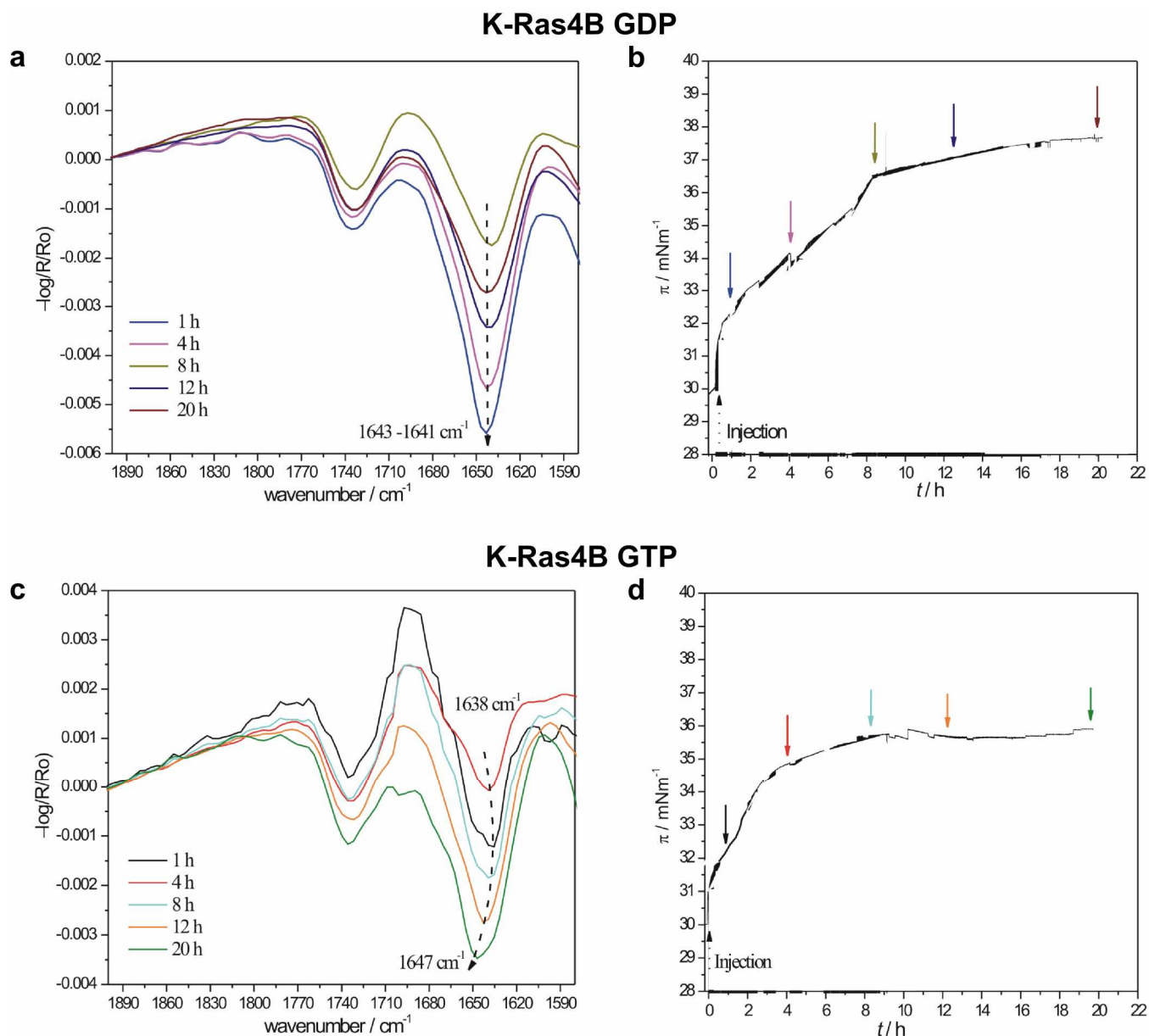
Figure S4. IRRA spectra of the amide-I′ region of K-Ras4B (a, c) at the respective positions of the surface pressure versus time curve (b, d). All spectra were recorded at an angle of incidence of 35° with p-polarized light. The initial surface pressure of the lipid monolayer consisting of DOPC/DOPG/DPPC/DPPG/Chol 20:5:45:5:25 was set to 30 mN m^{-1} before injection of the protein solution, since this surface pressure reflects the lipid density generally found in physiological lipid bilayers. After protein injection underneath the lipid monolayer into the subphase of the Langmuir through (protein concentration: 200 nM), the surface pressure increased immediately, indicating the protein′s surface activity. The time evolution of the surface pressure shows that the adsorption of K-Ras4B GTP is much faster compared to K-Ras4B GDP, suggesting a higher membrane affinity of K-Ras4B GTP. The amide-I′ band maximum around 1647 cm^{-1} points towards a more random orientation of the GTP-loaded protein inserted into the lipid monolayer.[S3]
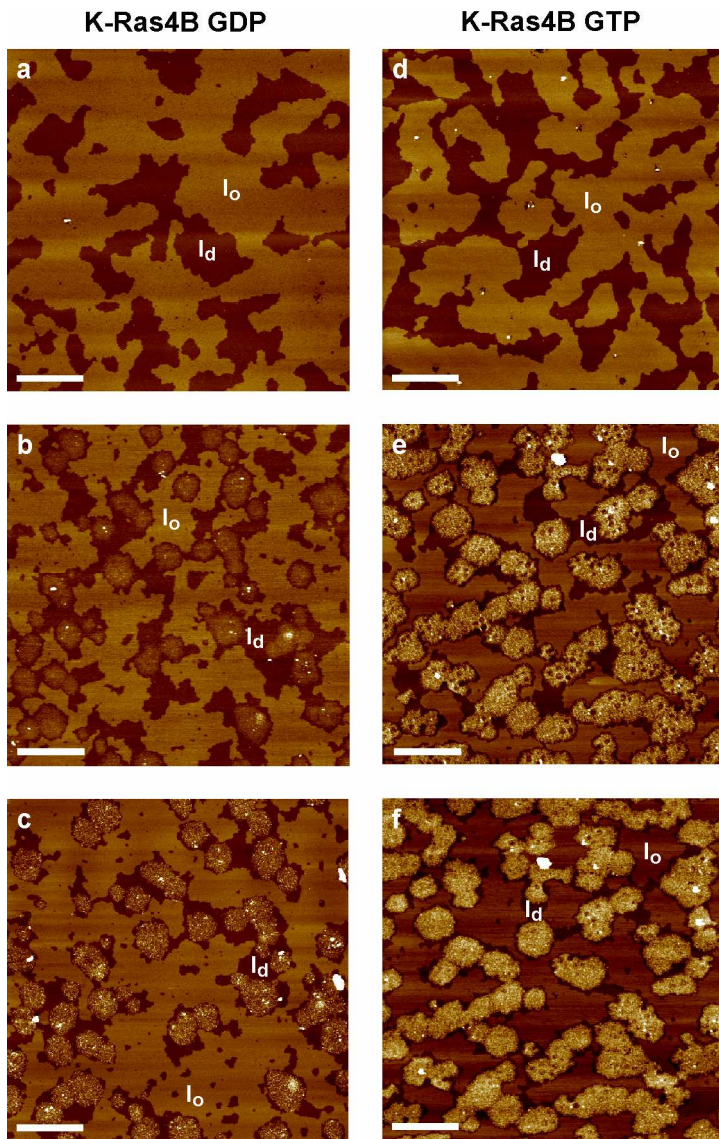
Figure S5. AFM images of the time-dependent partitioning of GDP- and GTP-loaded K-Ras4B into zwitterionic lipid bilayers consisting of DOPC/DPPC/Chol 25:50:25. The AFM images are shown before (a and d) and at particular time points ($t \approx 2$ and 3 h, b and e, respectively; $t \approx 23$ and 24 h, c and f, respectively) after injection of 200 μL of K-Ras4B in 20 mM Tris, 7 mM MgCl$_2$, pH 7.4 ($c_{\text{K-Ras4B}} = 2$ μM) into the AFM fluid cell. The overall height of the vertical color scale from dark brown to white corresponds to 6 nm for all images. The scale bar represents 2 μm.

K-Ras4B GDP

K-Ras4B GTP

0.952 nm   2.378 nm   0.775 nm

1.784 nm   1.087 nm   2.847 nm
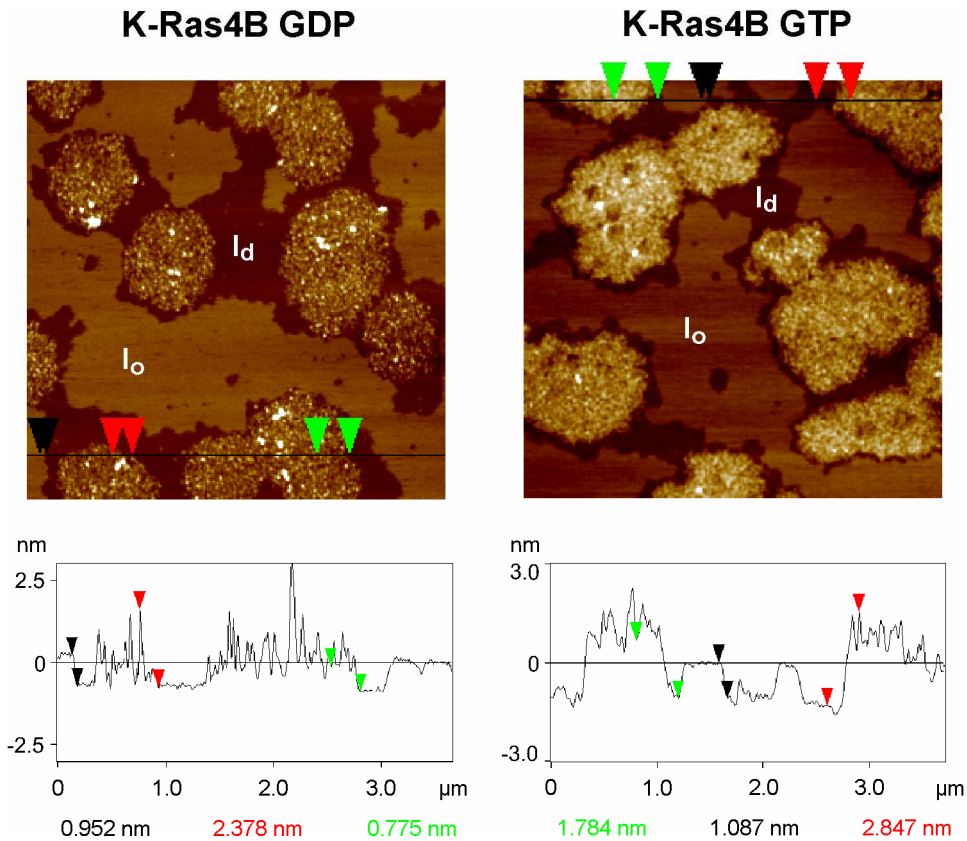
Figure S6. Analysis of the AFM images of GDP- and GTP-loaded K-Ras4B in zwitterionic hetero-geneous membranes. Zoom of the upper and middle right area of the AFM images at $t \approx 23$ and 24 h (c and f, respectively) in Fig. S2 and analysis of the corresponding AFM images for K-Ras4B GDP (left) and K-Ras4B GTP (right) ($c_{K-Ras4B} = 2$ μM). In the upper part, the section profiles of the AFM images are shown with a vertical color scale from dark brown to white corresponding to an overall height of 6 nm. The horizontal black line is the localization of the section analysis given at the bottom, indicating the vertical distances between pairs of arrows (black: l_o/l_d phase difference, green: thickness difference of the new domains enriched in K-Ras4B compared to l_d domains, and red: size of the K-Ras4B proteins). The AFM analysis revealed a mean height of 2.3 ± 0.4 nm ($n = 225$) for the inactive K-Ras4B proteins and a value of 2.8 ± 0.4 nm ($n = 217$) for the GTP-loaded K-Ras4B proteins. The new domains enriched in GDP- and GTP-loaded K-Ras4B exhibit a thickness that is 0.7 ± 0.1 nm ($n = 54$) and 1.8 ± 0.2 nm ($n = 43$) larger than that of the purely fluid lipid phase for the GDP and GTP bound state, respectively.

Materials and Methods

Materials and sample preparation. The phospholipids 1,2-dioleoyl-*sn*-glycero-3-phosphocholine (DOPC), 1,2-dioleoyl-*sn*-glycero-3-phospho-(1'-*rac*-glycerol) sodium salt (DOPG), 1,2-dipalmitoyl-*sn*-glycero-3-phospho-(1'-*rac*-glycerol) sodium salt (DPPG), and 1,2-dipalmitoyl-*sn*-glycero-3-phosphocholine (DPPC) were purchased from Avanti Polar Lipids (Alabaster, AL). Cholesterol (Chol) was from Sigma-Aldrich and the fluorescent lipids *N*-(lissamine rhodamine B sulfonyl)-1,2-dihexadecanoyl-*sn*-glycero-3-phosphoethanolamine triethylammonium salt (*N*-Rh-DHPE), 4,4-difluoro-5,7-dimethyl-4-bora-3a,4a-diaza-*s*-indacene-3-propionic acid, succinimidyl ester (BODIPY® FL, SE), and octadecylrhodamine B chloride (R18) from Molecular Probes (Invitrogen). All other reagents and solvents were obtained from Sigma-Aldrich and Merck. Stock solutions of 10 and 5 mg mL^{-1} lipid (DOPC, DOPG, DPPC, DPPG, and Chol) in chloroform were prepared and mixed to obtain 1.94 and 1.5 mg of total lipid with the desired composition of DOPC/DOPG/DPPC/DPPG/Chol 20:5:45:5:25 (molar ratio) for the AFM and FTIR experiments, respectively. The majority of the chloroform was evaporated with a nitrogen stream; all solvent was subsequently removed by drying under vacuum overnight. All buffers were filtered through filters of 0.02 μm pore size (Whatman, Dassel, Germany) before use.

Protein synthesis. The synthesis of the K-Ras4B proteins is described in detail in ref. S4. Briefly, the *S*-farnesylated K-Ras4B protein was synthesized by a combination of expressed protein ligation (EPL) and lipopeptide synthesis. The K-Ras4B peptide, possessing an additional cysteine at the *N*-terminus required for protein ligation, with the amino acid sequence H-Cys(S*t*Bu)-Lys$_6$-Ser-Lys-Thr-Lys-Cys(Far)-OMe was synthesized on a 2-chlorotrityl resin. After cleavage from the solid support, the peptide was purified and ligated to a truncated K-Ras4B protein core thioester, that was generated via expression in Impact™ vector pTWIN2 (New England Biolabs) and subsequent transformation of the resulting plasmid into *E.coli* BL21(DE3) cells. This yields a ligated K-Ras4B protein bearing an additional cysteine between Gly^{174} and Lys^{175}. The truncated K-Ras4B thioester was labeled with BODIPY prior ligation. For the synthesis of the K-Ras4B GTP, a nucleotide exchange step was introduce after BODIPY labeling of the protein core thioester. Subsequent ligation of the GTP loaded K-Ras4B protein core thioester to the corresponding peptide yielded the desired K-Ras4B GTP protein.

Cloning, expression and purification of K-Ras4BΔ15-MESNA thioester. The DNA sequence for the first 174 amino acids of human K-Ras4B was cloned from the according ptac vector into the pTWIN2-vector of the Impact™ system (NEB), *E. coli* Bl21(DE3) were transformed with the Ras-Intein-CBD plasmid and expression of the protein was performed at 20 °C. After harvesting of the bacteria the cells were lysed by ultrasonification in lysis buffer (20 mM Na-Hepes, pH 7.0, 500 mM

NaCl, 1 mM $MgCl_2$, 0.1% (v/v) Triton-X 100) and the soluble fraction was diluted to 500 mL of lysis buffer and applied to a chitin beads affinity column, after equilibration of the column with buffer (20 mM Na-Hepes, pH 7.0, 500 mM NaCl, 1 mM $MgCl_2$). After washing the column with equilibration buffer, the intein splicing was introduced by incubation of the column with intein-splicing buffer (20 mM Na-Hepes, pH 8.5, 50 mM NaCl, 1 mM $MgCl_2$, 100 mM MESNA) for 24 h at 4 °C. The K-Ras4BΔ15-MESNA thioester was washed from the column with intein-splicing buffer and concentrated by size exclusion filtration (Amicon Ultra-15 MWCO 10 kD, Millipore).

BODIPY labeling of the protein core thioester was performed as follows: The K-Ras4BΔ15-MESNA thioester was buffered in a 100 mM solution of $NaHCO_3$, pH 7.0 and a 10× excess of BODIPY-NHS was added. The mixture was shaken for 2 h at 4 °C under argon. After this time, labeled protein was purified using a Hi-Trap desalting column (5 mL, GE Healthcare) and concentrated. The fluorescence/protein ratio was determined by measuring the absorbance at 504 nm and at 280 nm, respectively.

Nucleotide exchange on Ras proteins was performed as follows: BODIPY-labeled or non labeled K-Ras4BΔ15-MESNA was incubated overnight at 4 °C with a two-fold molar excess of GppNHp in 20 mM Tris-HCl, 100 mM $(NH_4)_2SO_4$, 0.1 mM $ZnC1_2$ (pH 7.6), and alkaline phosphatase (Roche) at a concentration of 5 units/mg of Ras. After that, the buffer was exchanged for 20 mM Tris, 5 mM $MgCl_2$ (pH 7.5) using a Hi-Trap (GE Healthcare) desalting column. The sample was analyzed by reverse phase HPLC using 100 mM tetrabutylammonium bromide, 100 mM K_2PO_4, 0.2 mM NaN_3 (pH 6.4) in 7.5% acetonitrile. After aliquotation the protein was shock frozen and stored at -80 °C.

Ligation of K-Ras4B peptide with K-Ras4BΔ15-MESNA thioester. In an argon atmosphere K-Ras4B peptide was dissolved in buffer (100 mM Tris, 50 mM NaCl, 5 mM $MgCl_2$, 5 mM MESNA, pH 8.5) at 25 °C and the peptide was deprotected by adding 5 mM tris(2-chloroethyl)phosphate. After 5 minutes incubation, BODIPY labeled or non labeled-K-Ras4BΔ15-MESNA thioester (GDP or GTP) was added and placed on a mechanical stirrer for 3 hours. The reaction mixture was diluted 1:1 with buffer (25 mM NaAc, 1 mM $MgCl_2$, pH 5.4) and dialyzed overnight in buffer (25 mM NaAc, 1 mM $MgCl_2$, pH 5.4). Purification was done with a Hi-Trap SP-Xl (1 ml, GE Healthcare). The column was equilibrated with buffer (25 mM NaAc, 1 mM MgCl2, pH 6.3) and the protein solution was applied to the column and the column was washed with ten column volumes with the same buffer. The protein was released by washing with high salt buffer (25 mM NaAc, 500 mM NaCl, 1 mM $MgCl_2$, pH 6.3). Protein containing fractions were identified by mini Bradford assay and were concentrated by size exclusion filtration (Amicon Ultra-15 MWCO 10 kD, Millipore), and protein concentration was determined via Bradford assay. The protein was characterized using SDS-PAGE and MALDI. After aliquotation, the protein was shock frozen and stored at -80 °C.

Atomic force microscopy (AFM). The dry lipid mixture was hydrated with 1 mL of 20 mM Tris, 7 mM MgCl$_2$, pH 7.4. Details of the preparation of the supported lipid bilayers and the AFM setup are described in ref. S1. Briefly, vesicle fusion on mica was carried out by depositing 30 μL of the extruded lipid vesicle solution together with 40 μL of Tris buffer on freshly cleaved mica and incubation in a wet chamber at 70 °C for 2 h. For the protein–membrane interaction studies, 200 μL of K-Ras protein in Tris buffer ($c_{protein} = 2$ μM) were slowly injected into the AFM fluid cell at room temperature and allowed to incubate for 1 h. Afterwards, the fluid cell was rinsed carefully with Tris buffer before imaging to remove unbound protein.

Measurements were performed on a MultiMode scanning probe microscope with a NanoScope IIIa controller (Digital Instruments, Santa Barbara, CA) and usage of a J-Scanner (scan size 125 μm). Images were obtained by applying the tapping mode in liquid with oxide-sharpened silicon nitride (DNP-S) or sharp nitride lever (SNL) probes mounted in a fluid cell (MTFML, Veeco, Mannheim, Germany). Tips with nominal force constants of 0.32 N m^{-1} were used at driving frequencies around 9 kHz and drive amplitudes between 80 and 550 mV; scan frequencies were between 0.5 and 1.0 Hz.

Confocal laser scanning microscopy of model membranes. Stock solutions of 10 mg mL^{-1} lipid (DOPC, DOPG, DPPC, DPPG, and Chol) in chloroform/methanol 3:1 (v/v) were prepared and mixed to obtain 200 μL lipid mixture with the desired composition of DOPC/DOPG/DPPC/DPPG/ Chol 15:10:40:10:25 (molar ratio), into which 6 μL of a 1 mM *N*-Rh-DHPE chloroform stock solution were added, giving a final molar ratio of lipid/*N*-Rh-DHPE of 500:1. This sample was diluted with chloroform to a concentration of the lipid mixture solution of 4 mg mL^{-1}. GUVs were prepared by electroformation [S5–S7] in a temperature controlled home-made chamber (similar to the closed bath perfusion chamber RC-21 from Warner Instruments Co., Massachussets, USA) on optically transparent and electrically conductive indium tin oxide (ITO) coated glass slides (SPI Supplies, West Chester, USA). The BODIPY-labeled K-Ras4B proteins were added via an injection-channel ($c_{K-Ras4B} = 0.1{-}0.2$ μM), yielding a final BODIPY concentration in the cell-chamber of 10 nM.

Images were recorded by a confocal laser scanning microscope (Biorad MRC 1024, extended for multiphoton excitation, now Zeiss, Germany) coupled via a side-port to an inverted microscope (Nikon, Eclipse TE-300 DV, infinity corrected optics) enabling fluorescence excitation in the focal plane of an objective lens (Nikon Plan Fluor 40×, NA = 0.6, extra long working distance 3.7 mm and Nikon Plan Appochromat VC 60× A WI, NA = 1.2 collar rim corr.). Fluorescence in the green and red PMT-channels (emission band pass filters 522 nm/FWHM 35 nm and 580 nm/FWHM 40 nm, respectively) were sequentially acquired by alternating the excitation with the 488 and 568 nm lines of a Kr–Ar-laser

(Portmann Instruments AG, Biel-Benken, Switzerland). Image acquisition was controlled by the software LaserSharp2000 (formerly Biorad, now Zeiss).

FTIR spectroscopy. For the infrared spectroscopic experiments, the dry lipid mixture was hydrated with 100 μL of 20 mM Tris, 7 mM $MgCl_2$, pD 7.4, sonicated at 70 °C for 10 min and subsequently subjected to five freeze-thaw-vortex cycles. Afterwards, unilamellar vesicles of homogeneous sizes were obtained by using an extruder (Avanti Polar Lipids, Alabaster, AL) with polycarbonate membranes of 100 nm pore size at 70 °C. For the protein-lipid interaction studies, the GDP- and GTP-loaded K-Ras4B protein ($c = 100$ μg) was lyophilized for 3 h to remove H_2O and afterward 20 μL of the freshly extruded lipid mixture were added ($c_{K-Ras} = 233$ μM). The FTIR cell was then assembled and spectra collection started .

Measurements were performed at 25 °C with a Nicolet 5700 FTIR spectrometer equipped with a liquid nitrogen cooled MCT (HgCdTe) detector and a cell with CaF_2 windows that are separated by 50 μm mylar spacers. The spectrometer was purged continuously with dry air to remove water vapor. Typically, FTIR-spectra of 128 scans were taken with a resolution of 2 cm^{-1} and corresponding processing was performed using GRAMS software (Thermo Electron). After background subtraction, the spectra were baseline corrected and normalized by setting the area between 1700 and 1600 cm^{-1} to 1 to allow for a quantitative analysis of the time evolution of secondary structural changes.

For the analysis of the secondary structure changes, second derivative and Fourier self deconvolution (FSD) were applied to the normalized spectra to identify the components of the amide-I′ band region. These peaks were then fitted to the normalized raw spectra using a Levenberg-Marquardt curve fitting routine with bands of Voigt line shape. All spectra were fitted with similar set of peaks and parameters. In ambiguous cases (such as the overlap of unordered and α-helical band regions), information from NMR and X-ray diffraction was taken into account. [S8] The area under each peak represents the fraction of the respective component (assuming similar transition dipole moments for the different conformers) and was finally used to determine the percentages of the secondary structure components.

Infrared reflection absorption (IRRA) spectroscopy. All experiments were performed with a Wilhelmy film balance (Riegler, Berlin, Germany) using a filter paper as Wilhelmy plate. Two teflon troughs of different sizes were linked by two small bores to ensure equal heights of the air-D_2O interface in both troughs. The temperature of the subphase was maintained at 20 ± 0.5°C and measurements were performed in the small (reference) trough at constant surface area. A Plexiglas hood covered the entire reflection attachment to minimize the evaporation of subphase. Both troughs were filled with 100 mM NaCl in D_2O. Monolayers of DOPC/DOPG/DPPC/DPPG/Chol (20:5:45:5:25) were

formed by directly spreading the lipid solution (1 mM) in a mixture of chloroform and methanol (3:1) onto the subphase. Protein adsorption measurements were performed by injection of a concentrated protein solution into the subphase below the monolayers to yield a concentration of 200 nM..

Infrared spectra were recorded using a Vertex 70 FT-IR spectrometer (Bruker, Germany) connected to an A511 reflection attachment (Bruker) with an MCT detector using the trough system described above. The IR beam is focused by several mirrors onto the subphase and the trough system was positioned on a movable platform to be able to shuttle between sample and reference troughs. This shuttle technique diminishes the spectral interference due to water vapour absorption in the light beam. Parallel polarized light at an angle of incidence of 35° was used for recording of the IRRA spectra. All spectra were recorded at a spectral resolution of 8 cm^{-1} using Blackman-Harris-3-term apodization and a zero filling factor of 2. For each spectrum 2000 scans were co-added. The single beam reflectance spectrum of the big trough was ratioed as background (R_o) to the single beam reflectance spectrum of the lipid monolayer on the reference trough (R) to calculate the reflection absorption spectrum as $-\log(R/R_o)$.

References

(S1) Weise, K.; Triola, G.; Brunsveld, L.; Waldmann, H.; Winter, R. *J. Am. Chem. Soc.* **2009**, *131*, 1557–1564.

(S2) Rinia, H. A.; Snel, M. M. E.; Van der Eerden, J. P. J. M.; de Kruijff, B. *FEBS Lett.* **2001**, *501*, 92–96.

(S3) Meister, A.; Nicolini, C.; Waldmann, H.; Kuhlmann, J.; Kerth, A.; Winter, R.; Blume, A. *Biophys. J.* **2006**, *91*, 1388–1401.

(S4) Chen, Y.-X.; Koch, S.; Uhlenbrock, K.; Weise, K.; Das, D.; Gremer, L.; Brunsveld, L.; Wittinghofer, A.; Winter, R.; Triola, G.; Waldmann, H. *Angew. Chem. Int. Ed.* **2010**, *49*, 6090–6095.

(S5) Nicolini, C.; Baranski, J.; Schlummer, S.; Palomo, J.; Burgues, M. L.; Kahms, M.; Kuhlmann, J.; Sanchez, S.; Gratton, E.; Waldmann, H.; Winter, R. *J. Am. Chem. Soc.* **2006**, *128*, 192–201.

(S6) Angelova, M. I.; Soleau, S.; Meleard, P.; Faucon, F.; Bothorel, P. *Prog. Colloid Polym. Sci.* **1992**, *89*, 127–131.

(S7) Janosch, S.; Nicolini, C.; Ludolph, B.; Peters, C.; Völkert, M.; Hazlet, T.L.; Gratton, E.; Waldmann, H.; Winter, R. *J. Am. Chem. Soc.* **2004**, *126*, 7496–7503.

(S8) Milburn, M. V.; Tong, L.; deVos, A. M.; Brünger, A.; Yamaizumi, Z.; Nishimura, S.; Kim, S. H. *Science* **1990**, *247*, 939–945.

Complete reference 16 and 36:

(16) Bivona, T. G.; Quatela, S. E.; Bodemann, B. O.; Ahearn, I. M.; Soskis, M. J.; Mor, A.; Miura, J.; Wiener, H. H.; Wright, L.; Saba, S. G.; Yim, D.; Fein, A.; Pérez de Castro, I.; Li, C.; Thompson, C. B.; Cox, A. D.; Philips, M. R. *Mol. Cell* **2006**, *21*, 481–493.

(36) Dekker, F. J.; Rocks, O.; Vartak, N.; Menninger, S.; Hedberg, C.; Balamurugan, R.; Wetzel, S.; Renner, S.; Gerauer, M.; Schölermann, B.; Rusch, M.; Kramer, J. W.; Rauh, D.; Coates, G. W.; Brunsveld, L.; Bastiaens, P. I.; Waldmann, H. *Nat. Chem. Biol.* **2010**, 6, 449–456.